

OptiKit: An Open Source Kit for Simulation of On-Chip Optical Components

Eldhose Peter, Smruti R. Sarangi

Department of Computer Science and Engineering, IIT Delhi

{csz138108,srsarangi}@cse.iitd.ac.in

Abstract—This paper presents the design of OptiKit – an open source kit for simulating passive optical devices in embedded photonics based chips. OptiKit includes models for waveguides, parallel waveguides, multiple MMI devices, Y junctions, directional couplers, and waveguide bends. We describe the structure, basic physics, possible applications of each device, and the details of the devices included in OptiKit. Each device has been optimized for performance, and power, and has been tuned appropriately. All the devices can be simulated using the optical simulation software, RSoft, and its results can subsequently be incorporated in a traditional EDA based flow.

I. INTRODUCTION

On-chip optical communication technology is beginning to be recognized as a promising alternative to standard on-chip interconnects. As compared to traditional copper based interconnects, optical interconnects are faster [1], more power efficient [1], and can sustain an order of magnitude more bandwidth [2]. They can also be used for novel applications such as switching, and fast on-chip broadcast [2]. Consequently, researchers in the field of computer architecture have begun to design prototype systems using optical interconnects, and have reported promising gains. In specific, researchers have looked at fast inter cache bank communication [3], [4], high speed cache invalidation [2], [5], and ultra fast barrier synchronization [6] using optical interconnects. Simultaneously, the device physics community has made great strides in fabricating optical devices, and using them for on-chip transmission in small test chips. They have shown that it is possible to fabricate highly reliable, and fast optical devices that can switch at multi-gigahertz frequencies [7], [8].

We are now at an interesting juncture in time. Optical technologies have already proved their worth in off chip technologies and are currently being used for communication across multiple boards in clusters, and for telecommunication networks. According to Intel’s roadmap, optical technology is expected to be used in chips sometime after 2016. A recent paper published by HP labs [2] already talks about passive optical devices that have been fabricated by HP, and their commercial viability. We thus see that the architecture, and the device physics communities have made great strides in using and integrating optical technology.

We believe that the time has come for the EDA and VLSI communities to look at optical technology seriously. We counted, the number of papers in the premier EDA conferences (DAC, ICCAD, DATE, ASPDAC, VLSI) in the area of on-chip optical technology, and we found only 8 references. There were 3 papers on the design of optical routers, 4 papers on optical network topologies, and 1 paper on routing with

optical interconnects [9]. However, the traditional VLSI/ EDA problems of floorplanning, placement, routing, compaction, verification, reliability, and design for debug remain unsolved in this domain. For example, with the increased integration of on-chip optical interconnects, it will be necessary to design sophisticated routing algorithms to minimize the lengths of optical waveguides(optical channels), the number of bends, and consequently minimize the optical power loss as pointed out in [9]. Traditional EDA problems are still valid in this new domain, albeit with added constraints.

A major hindrance to conducting research in this area, is the lack of simulation tools, and widely available models for optical components, and associated infrastructure. In this paper, we describe the design of a soon to be released open source kit(OptiKit), which contains a set of models of passive optical devices. OptiKit contains the models of most commonly used passive optical devices that have been used in literature. These models can be simulated, modified, and tuned using the widely used optical simulator, Synopsys RSoft. Note that these devices are not natively supported by RSoft, and it takes a significant amount of effort to make them functional. OptiKit can thus reduce the effort of the user, and further make it possible for EDA researchers to use the models of devices that we provide, to build large optical circuits by interconnecting them. These circuits can later on be optimized for different criteria such as power, reliability, and performance, using a host of novel EDA algorithms.

We discuss some theoretical preliminaries in Section II, and in Section III describe the operation, basic physics, thumb rules, and design of a set of passive optical devices – waveguide, Y-junction, directional coupler, MMI, waveguide bend, and ring resonator.

II. PRELIMINARIES

A. Fundamentals of Electro-Magnetism

The propagation of an electro-magnetic wave is governed by the Maxwell’s equations:

$$\nabla \cdot \mathbf{E} = \frac{\rho}{\epsilon_0} \quad (1) \quad \nabla \times \mathbf{E} = -\frac{\partial \mathbf{B}}{\partial t} \quad (3)$$

$$\nabla \cdot \mathbf{B} = 0 \quad (2) \quad \nabla \times \mathbf{B} = \mu_0 \mathbf{J} + \mu_0 \epsilon_0 \frac{\partial \mathbf{E}}{\partial t} \quad (4)$$

Here, μ_0 and ϵ_0 are the permeability and permittivity of free space respectively. \mathbf{E} , and \mathbf{B} are the electrical and magnetic fields, and \mathbf{J} is the current density. ρ is the charge density. For an on-chip optical interconnect in which light travels within a constrained medium, $\rho = 0$, and the electro-magnetic fields outside the medium are 0. This leads to a simpler formulation

of the Maxwell's equations, and is solved by primarily two methods – BeamProp, and FDTD.

The beam propagation(BeamProp) method assumes that the solution to the Maxwell's equation follows the *slowly varying envelope* approximation. This means that the variation of the amplitude of the solution is very small as compared to the variation in the phase, and distance of propagation. This is a fast method, and is applicable to structures whose physical properties vary slowly with the geometry. Structures with sharp features cannot be simulated using this method.

The FDTD (finite difference time domain) method uses the standard finite difference method to solve the Maxwell's equations. It is also known as the *full wave* method. It discretizes the equations, and solves them using linear algebraic techniques. To accelerate finite difference methods, standard approaches such as Krylov subspace based model order reduction, and multigrid analysis are used. It can be used for all types of structures. As compared to BeamProp it is at least an order of magnitude slower.

B. Waveguide

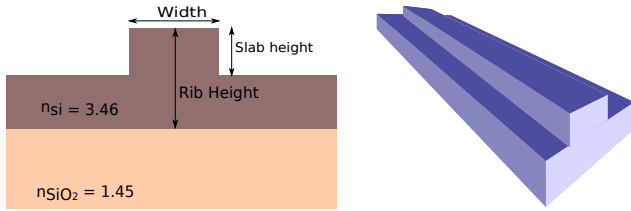


Fig. 1: A rib waveguide

Light travels in a medium known as a *waveguide*. Figure 1 shows the cross sectional view of a SOI(*Silicon On Insulator*) rib waveguide. The core of the waveguide is typically made of silicon or a polymer. We use silicon based waveguides with a refractive index of 3.46. The refractive index of the surrounding cladding (made of SiO_2) is typically 1.45. Light remains confined to the waveguide because of total internal reflection, owing to the fact that its refractive index is significantly greater than that of the surroundings. We can also have slab shaped waveguides; however, rib waveguides are better for on-chip interconnects [10], [11].

The mode of propagation of light in a waveguide can be classified into the following categories.

- *Transverse Electric (TE) Mode*: The component of the electric field along the direction of propagation is 0.
- *Transverse Magnetic (TM) Mode*: The component of the magnetic field along the direction of propagation is 0.
- *Transverse Electric and Magnetic (TEM) Mode*: Combination of TE and TM.
- *Hybrid Mode*: There is a non-zero amount of field in the direction of propagation.

C. A Typical Optical Communication System

Figure 2(a) shows the diagram of a typical on-chip communication system. The light source is typically an off-chip laser, or an on-chip VCSEL based laser. In either case, they are typically silicon based lasers that produce light at a

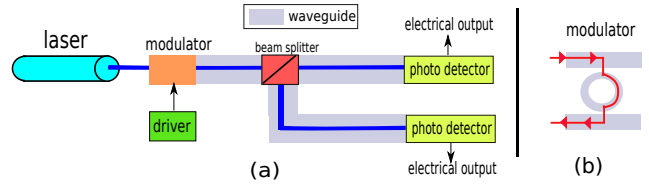


Fig. 2: An on-chip optical communication system

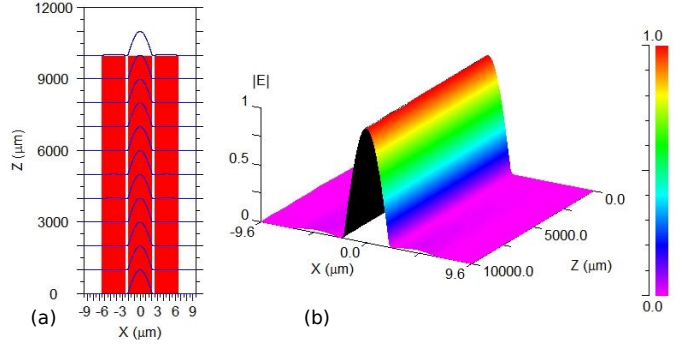


Fig. 3: Simulation of parallel waveguides

wavelength of 1550 nm. The laser power is modulated, by a ring based modulator as shown in Figure 2(b). If it is in resonance, then it couples all the light out of the waveguide, and when it is off resonance, it allows light to pass through. It is possible to bring it in and out of resonance by altering its refractive index with the application of a tiny amount of electric charge. Light propagates along the waveguide, and can be transferred to other waveguides using beam splitters that transfer a fixed fraction of light. The photo detectors at the end of the waveguides detect the amplitude of light and use a set of trans-impedance amplifiers to amplify the signal. Owing to the fact that photons are Bosons, they typically cannot be stored or confined to small spaces as is the case with electrons. Hence, we cannot build optical capacitors, or other photon storage based optical devices. Almost all devices that are used in on-chip photonics are primarily passive devices that just modify the flow of the direction of light, or split the signal.

III. OPTICAL COMPONENTS

In this section, we present the physics, and design of six passive optical structures. We refer to [12] for most of our equations, and design choices. We use Synopsys RSoft 8.0.2.1 for our optical simulations. OptiKit should be compatible with most versions of RSoft.

A. Waveguides

We model rib based waveguides as shown in Figure 1. The user can change the width, height, and rib height to suit her needs. The user however needs to be cautious with the placement of parallel waveguides. If they are too close, we risk unwanted interference. Figure 3 shows an example. We place three $4 \mu\text{m}$ wide waveguides side by side, separated by $0.5 \mu\text{m}$. We observe some amount of coupling ($\approx 2\%$) in the other waveguides (refer to the small kinks in Figure 3(b)).

In the rest of the structures we use a standard rib waveguide with the parameters shown in Table I. Sometimes inside a

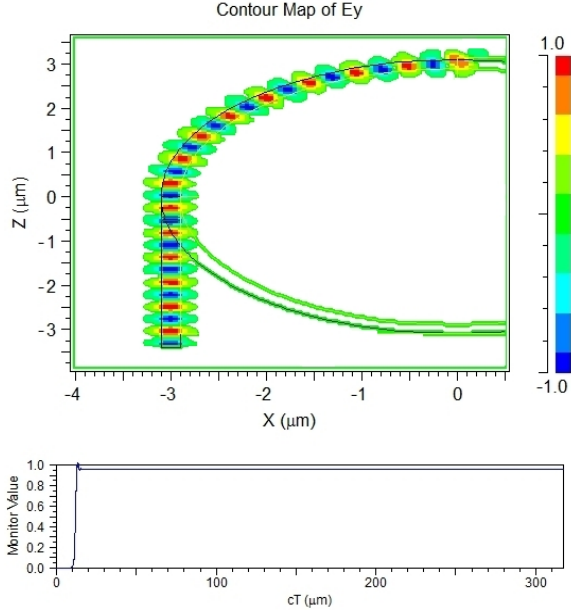


Fig. 4: Simulation of a 90° optical waveguide bend

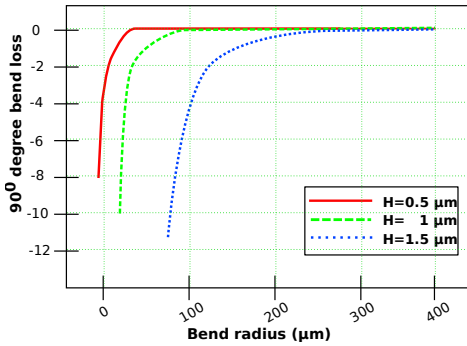


Fig. 5: dB loss of a waveguide bend (source [12])

structure, we need to vary the widths of the waveguides to minimize optical power loss. In this case, we add a set of tapers [12] to transfer optical power into and out of an optical device. A taper is a trapezoidal waveguide that connects waveguides of different widths.

B. Waveguide Bend

The right angled waveguide bend [13] is the most popular optical element. A bend in a waveguide allows us to change its direction. However, there is an associated loss in optical power. We support 90° bends. A *fullwave* simulation of a waveguide bend in RSoft is shown in Figure 4(a). Note the time taken for the signal to rise to the final value at the end of the bend in Figure 4(b). The main parameters of a bend are the inner radius, outer radius, rib width, rib height and etch depth.

Waveguide bends are prone to losses, mainly radiation loss as the optical signal propagates around the bend. As shown in Figure 5, the bend loss reduces when the bend radius increases. In a bent waveguide, the optical signal shifts outward and deviates from the center of the waveguide in a lateral direction. Using the conformal transformation method, we can consider the bend as a straight waveguide with equivalent width as given by Equation 5.

Parameters	Values
Waveguide	
width	$1 \mu\text{m}$
slab height	$0.75 \mu\text{m}$
rib height	$1.5 \mu\text{m}$
loss	1 dB/cm
simulation type	BeamProp
Waveguide Bend	
outer radius	$3.1 \mu\text{m}$
inner radius	$2.9 \mu\text{m}$
λ	$1.55 \mu\text{m}$
width of waveguide	$0.2 \mu\text{m}$
refractive index of waveguide	3.46
background refractive index	1.42
fdtd_time_step	$0.0125 \times \lambda$
fdtd_stop_time	$16384 \times \text{fdtd_time_step}$
monitor time	$8 \times \text{fdtd_time_step}$
simulation type	FDTD

TABLE I: Parameters of the waveguide bend

$$W_{equ} = R_2 \ln \frac{R_2}{R_1} \quad (5)$$

The equivalent refractive index profile is:

$$n_{equ}(u) = n(u)e^{\frac{u}{R_2}} \quad (6)$$

Here, R_2 and R_1 are the outer and inner radii respectively and $n(u)$ is the refractive index profile without bends.

A relatively minor source of optical power loss is the transition loss between the bent waveguide and the straight waveguide due to a mismatch in the modal profile. The transition loss [14] at the junction of the bent and straight waveguides is given by (in dB) [12]:

$$L_T = -10 \log \frac{\left| \int_{-\infty}^{\infty} \int_{-\infty}^{\infty} E_0(x, y) E_0^{B*}(x, y) dx dy \right|^2}{\left| \int_{-\infty}^{\infty} \int_{-\infty}^{\infty} E_0(x, y) E_0^*(x, y) dx dy \right|} \times \frac{1}{\left| \int_{-\infty}^{\infty} \int_{-\infty}^{\infty} E_0^B(x, y) E_0^{B*}(x, y) dx dy \right|} \quad (7)$$

Here $E_0(x, y)$ and $E_0^B(x, y)$ denote the modal fields for the straight and bent waveguides respectively and \star denotes the complex conjugation.

In our RSoft model of a bend, we have used two concentric lenses to make the curve, since a bend is not natively available in RSoft. The inner lens is made of an optically inactive material, resulting in the two lenses acting as a ring. Now, we *merge* $3/4^{\text{th}}$ of the ring with an inactive material layer. RSoft has a *merge* functionality, which allows us to demarcate regions made of an active material as inactive. The remaining $1/4^{\text{th}}$ of the ring is now a 90° bend. The dimensions of the simulated bend are shown in Table I :

C. 1×8 MMI

MMI [15] stands for Multimode Interference Coupler, and is most commonly used as a signal broadcast element. An MMI splits an optical signal into N parts, where each part is a copy of the original, albeit with a reduced amplitude. The light enters into the MMI through an input waveguide, and diffracts within the MMI. The diffracted waves reflect on the walls of the MMI and interfere to form high intensity

interference spots. The output waveguides are placed at these interference spots, and thus transfer optical energy out of the MMI device. To summarize, a $1 \times N$ MMI takes the optical signal as input through the input waveguide and replicates the signal with a reduced amplitude at N output channels.

Let W be the width and L be the length of MMI. The effective width W_{eff} of the MMI can be calculated as [12]:

$$W_{eff} = W + \frac{\lambda}{\pi} \left(\frac{n_c}{n_r} \right)^{2\sigma} (n_r^2 - n_c^2)^{-1/2} \quad (8)$$

Here, λ denotes the wavelength of the input signal, n_r and n_c are the refractive index of the core and cladding of the waveguide respectively. $\sigma = 0$ for the TE mode, and $\sigma = 1$ for the TM mode. The effective width will always be greater than the physical width because of the penetration of light into the cladding.

The beat length is defined as the distance at which the polarization rotates by 360 degrees.

$$L_\pi = \frac{4n_r W_{eff}^2}{3\lambda} \quad (9)$$

The main property of a $1 \times N$ MMI is that the M fold image is found at a distance of $\frac{3L_\pi}{4M}$ from the input port. Here, M represents the number of copies of the input signal. If we just want to create a mirror image, then the length of the MMI should be $\frac{3L_\pi}{4}$. If we want to create 8 copies, then the length should be $\frac{3L_\pi}{32}$. Equation 10 shows the relation for the length of the wave guide as a function of the beat length. k is a positive integer.

$$L = k \times \frac{3L_\pi}{4M} \quad (10)$$

For a $2N \times 2N$ MMI, the image of the input, or its mirror inverse is found at a distance of $k \times 3L_\pi$. The M fold images are found at a distance of $3kL_\pi/M$.

$$L = k \times \frac{3L_\pi}{M} \quad (11)$$

Thumb Rules: An MMI is a very flimsy device, and it needs to be designed cautiously. We need to first set the width of the MMI coupler. The width needs to be larger than the sum of the widths of all the input waveguides. We also need to insert some spacing between the waveguides. The width of the MMI is typically calculated by assuming that we require 5-10 μm per input waveguide. The length needs to satisfy Equations 8–11. For optimal values, the length is typically between 100-300 μm .

The MMI coupler can be used to split a signal into many signals. The fabricated 1x8 MMI has the parameters [7] shown in Table II, and its structure and simulation results are shown in Figure 6. The total optical loss of the constructed MMI device is around 0.98 dB. OptiKit 2.0 will have many more configurations of MMIs.

D. Directional Coupler

The *Directional Coupler* (DC) [8] is a set of two parallel waveguides that are kept in close proximity so that any optical signal that propagates through one waveguide can get transferred to the other. It is typically used as a beam splitter.

Parameter	Value
MMI Width(W)	48 μm
MMI length(L)	680 μm
separation between output waveguides(S)	6.2 μm
λ	1.55 μm
width of the rib waveguide(w)	3 μm
slab high	1 μm
rib high	3 μm
n_r	1.46
n_c	3.45
simulation type	BeamProp

TABLE II: Parameters for the MMI simulation

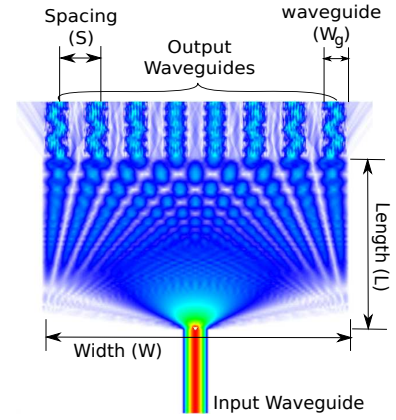


Fig. 6: Structure of 1x8 MMI

When the spacing between waveguides is small, the evanescent parts of the guided modes overlap and there is a net transfer of energy due to coupling. One waveguide induces a signal in the other waveguide, which in turn induces a coupling in the former waveguide, and the process continues recursively.

The coupling between two guided signals a and b can be described using an approximate solution to the wave equation, which can be written as [12]:

$$E(r, t) = a(z)\epsilon_a(x, y)e^{i(\omega t - \beta_a z)} + b(z)\epsilon_b(x, y)e^{i(\omega t - \beta_b z)} \quad (12)$$

Here, $\epsilon_a(x, y)$ and $\epsilon_b(x, y)$ are the transverse spatial electric field distributions in both the waveguides. Here $a(z)$ and $b(z)$ are the amplitudes of the modes in waveguides a and b as functions of the longitudinal coordinates (see [16]). β_a and β_b are the propagation constants of the waveguides.

Figure 7 shows the RSoft simulation (details in Table III) of

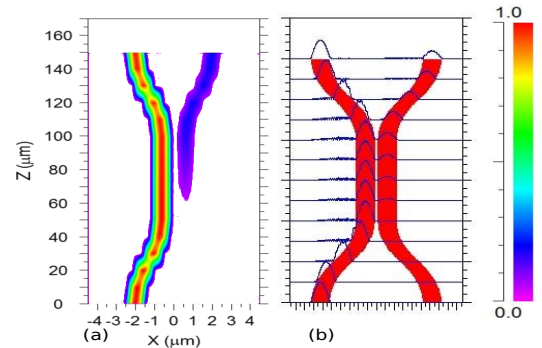


Fig. 7: Directional coupler

Parameters	Values
refractive index of waveguide	3.46
background refractive index	1.42
λ	$1.55\mu\text{m}$
length of each waveguide segment	$50\mu\text{m}$
width	$1\mu\text{m}$
separation	$0.25\mu\text{m}$
simulation type	BeamProp

TABLE III: Details of the directional coupler

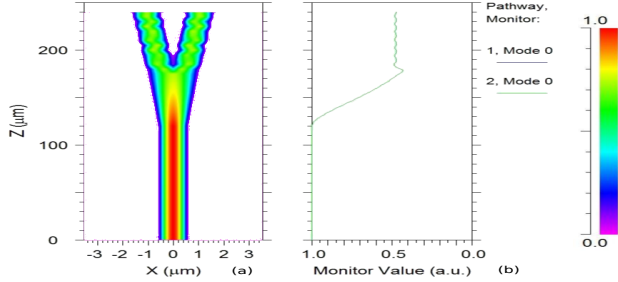


Fig. 8: Y junction

a directional coupler. Note the transfer of energy to the coupled waveguide. The optical loss of the fabricated coupler is 0.09 dB where the power at the output of the main waveguide is 84 % and the coupled output power is 14 %.

Thumb Rule: The user can modify the parameters of the directional coupler. However, she needs to note that the length of the coupled portion needs to be very long (at least 50-100 μm), and the separation should be typically less than 1 μm .

E. Y junction

The Y junction [17] is an optical structure in which either a single waveguide splits into two waveguides, or two waveguides combine to form a single waveguide. It is used as either a splitter or a combiner. It can either be symmetric, and split light equally, or it can be asymmetric and split unequally across the branches. There is a small amount of power loss, and the magnitude of the loss is directly proportional to the tip size (width of the intersection area of the inner surfaces of the branches) and opening angle (angle between the branches). The tip size cannot be 0 due to fabrication limitations. Secondly, if the opening angle is small, then the waveguides will become very narrow and light will escape.

The *Y junction* is a very effective beam splitter and can be used to multicast a signal from a single source to a set of destinations. Figure 8 shows the RSoft simulation of a symmetric Y junction, and its parameters are shown in Table IV. Figure 8(b) shows the intensity level of the optical signal as it is split into two equal parts. We measure an optical power loss of 10%.

Thumb Rules: The tip size should at least be equal to twice the width of the cladding, and the user needs to ensure that the opening angle is as small as possible. This will minimize the optical power loss.

F. Microring Resonator

A microring resonator [18] is a combination of two straight waveguides and a circular waveguide placed side by side

Parameters	Values
Refractive index of waveguide	3.46
background refractive index	1.42
λ	$1.55\mu\text{m}$
Width of waveguide	$1\mu\text{m}$
Angle of Y (rad)	0.8
simulation type	BeamProp

TABLE IV: Parameters for the Y junction simulation

as shown in Figure 10. The signal enters waveguide 1 via the *input port*, and if the structure is not in resonance then the signal leaves through the *through port* of waveguide 1. However, by applying a small electric change, it is possible to change the refractive index of the waveguides to bring the structure into resonance. In this case, light couples into the circular waveguide, and leaves through waveguide 2 via the *drop port*. Gradually, over time the amount of signal that gets coupled from waveguide 1 to waveguide 2 via the circular waveguide increases till almost the entire signal gets removed from waveguide 1. This is the point of *resonance*. Note that it is possible to take the resonator off resonance by slightly modifying the refractive indices of the waveguides. This can be done by applying a small amount of electrical change, or by a drastic change in the temperature.

A ring resonator is primarily used to modulate light on a waveguide because it has the capability to either remove 100% of the signal, or keep all of it flowing in the waveguide. It is also used in optical switches to transfer signals from one waveguide to another. A ring resonator is a fairly delicate structure, and is very sensitive to the wavelength of light. It can thus also be used to selectively transfer signals belonging to a certain wavelength.

The expression for the resonant wavelength of the ring is:

$$\lambda_r = \frac{2\pi R n_{eff}}{m} \quad (13)$$

Here, R is the radius of the resonator, m is an integer and n_{eff} is the effective refractive index of the ring (refer to Equation 6 and [12]). The coupling efficiency of waveguides is a major factor in the optical loss of the microring structure. Some amount of transmission loss occurs when light passes through the ring multiple times. For small waveguides, the roughness of the sidewalls and surfaces accounts for the transmission loss too.

In Figure 9, we show the *full wave* simulation of a microring resonator in RSoft. Light enters the structure through the waveguide in the left, and then the coupled signal rotates within the ring till the signal gets coupled with the output waveguide completely. Note the intensity of the optical signal at the upper end of the input waveguide and at the lower end of the output waveguide.

Since RSoft does not support microring resonators natively, we fabricated it using two lenses. They are kept in a concentric fashion, thus forming a ring of width $R_2 - R_1$, where R_2 is the outer radius and R_1 is the inner radius. The inner lens is made of inactive material. Two parallel waveguides are kept adjacent to this ring in the same plane, as shown in Figure 10. The microring resonator is designed with the values shown in Table V. The optical loss of the constructed ring is 0.45 dB,

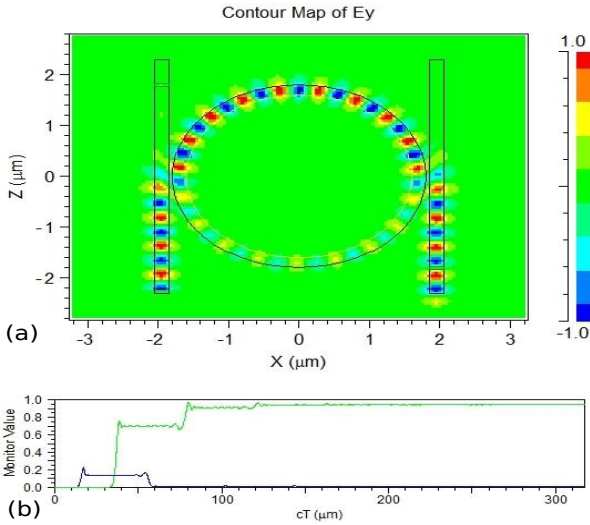


Fig. 9: Fullwave simulation of a microring resonator

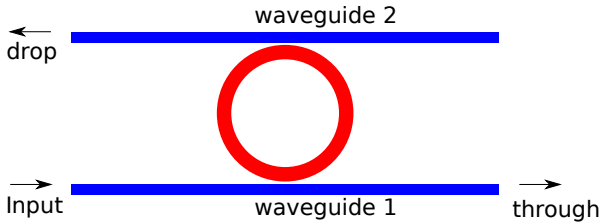


Fig. 10: Design of a microring resonator

and the power at the through port is negligible.

Traditionally, microring resonators have been considered to be very sensitive to temperature. However, with SOI technology, the temperature sensitivity is much lower because the difference in the refractive indices between the core and the cladding of the waveguides is more than that in bulk silicon. The calculated temperature sensitivity of the effective refractive index is $0.0003/\text{K}$, and we observed that even a temperature change of 30K did not take the resonator off resonance.

Thumb Rules: This is also a very delicate structure, and it takes a long time to design a structure that resonates and removes close to 100% of the power. The separation between the straight waveguides and the circular waveguide needs to

Parameter	Value
gap between ring and straight waveguide	$0.05\mu\text{m}$
outer radius of ring	$1.8\mu\text{m}$
inner radius of ring	$1.6\mu\text{m}$
λ	$1.55\mu\text{m}$
width of waveguide	$0.2\mu\text{m}$
height	$0.7\mu\text{m}$
slab height	$0.4\mu\text{m}$
refractive index of waveguide	3.46
background refractive index	1.42
fdtd_time_step	$0.0125 \times \lambda$
fdtd_stop_time	$2 \times 16384 \times \text{fdtd_time_step}$
monitor time	$8 \times \text{fdtd_time_step}$
simulation type	FDTD

TABLE V: Parameters for the microring resonator simulation

be very small (about $0.05\mu\text{m}$). The waveguide needs to be made narrower to about $0.2\mu\text{m}$, and appropriate tapers need to be added.

IV. SUMMARY AND DISCUSSION

In this paper, we presented the design of a toolkit called OptiKit that is scheduled to be released under an open source license to help EDA/VLSI researchers simulate optical circuits, and solve relevant EDA problems. We presented the devices as shown in Table VI along with their governing equations, and thumb rules to modify them if required.

Device	Utility
Waveguide	carry optical signals
Bend	bend the direction of light
MMI	achieve optical broadcast
DC	beam splitter
Y junction	beam splitter
ring resonator	optical switch/ modulator

TABLE VI: List of optical devices in OptiKit

REFERENCES

- [1] M. Haurylau, G. Chen, H. Chen, J. Zhang, N. A. Nelson, D. H. Albonese, E. G. Friedman, and P. M. Fauchet, "On-chip Optical Interconnect Roadmap: Challenges and Critical Directions," *Selected Topics in Quantum Electronics, IEEE Journal of*, vol. 12, no. 6, pp. 1699–1705, 2006.
- [2] D. Vantrease, R. Schreiber, M. Monchiero, M. McLaren, N. P. Joppi, M. Fiorentino, A. Davis, N. Binkert, R. G. Beausoleil, and J. H. Ahn, "Corona: System Implications of Emerging Nanophotonic Technology," ser. ISCA '08. IEEE Computer Society, 2008, pp. 153–164.
- [3] M. C. F. Chang, J. Cong, A. Kaplan, C. Liu, M. Naik, J. Premkumar, G. Reinman, E. Socher, and S.-W. Tam, "Power reduction of CMP communication networks via RF-interconnects," ser. MICRO 41. IEEE Computer Society, 2008, pp. 376–387.
- [4] N. Kirman and J. F. Martínez, "A power-efficient All-optical On-chip Interconnect Using Wavelength-based Oblivious Routing," ser. ASPLOS XV. ACM, 2010, pp. 15–28.
- [5] N. Kirman, M. Kirman, R. K. Dokania, J. F. Martinez, A. B. Apsel, M. A. Watkins, and D. H. Albonese, "Leveraging Optical Technology in Future Bus-based Chip Multiprocessors," ser. MICRO 39, 2006, pp. 492–503.
- [6] N. Binkert, A. Davis, M. Lipasti, R. Schreiber, and D. Vantrease, "Nanophotonic Barriers," in *Workshop on Photonic Interconnects & Computer Architecture (in conjunction with MICRO 41)*, 2009, pp. 1–4.
- [7] P. Trinh, S. Yegnanarayanan, F. Coppinger, and B. Jalali, "Compact multimode interference couplers in silicon-on-insulator technology," in *Lasers and Electro-Optics, 1997. CLEO '97., Summaries of Papers Presented at the Conference, 1997*, p. 441.
- [8] P. Trinh, S. Yegnanarayanan, and B. Jalali, "Integrated optical directional couplers in silicon-on-insulator," *Electronics Letters*, vol. 31, no. 24, pp. 2097–2098, 1995.
- [9] C. Condrat, P. Kalla, and S. Blair, "Crossing-Aware Channel Routing for Photonic Waveguides," 2013.
- [10] L. Vivien, F. Grillot, E. Cassan, D. Pascal, S. Lardenois, A. Lupu, S. Laval, M. Heitzmann, and J.-M. Fédéli, "Comparison between strip and rib SOI microwaveguides for intra-chip light distribution," *Optical Materials*, vol. 27, no. 5, pp. 756–762, 2005.
- [11] D. R. Lim, "Device Integration for Silicon Microphotonic Platforms," Ph.D. dissertation, Massachusetts Institute of Technology, 2000.
- [12] G. T. Reed, *Silicon Photonics: The State of the Art*. John Wiley & Sons, 2008.
- [13] Y. A. Vlasov, S. J. McNab *et al.*, "Losses in single-mode silicon-on-insulator strip waveguides and bends," *Opt. Express*, vol. 12, no. 8, pp. 1622–1631, 2004.
- [14] D. Dai and S. He, "Analysis of characteristics of bent rib waveguides," *J. Opt. Soc. Am. A*, vol. 21, no. 1, pp. 113–121, Jan 2004.
- [15] L. Soldano and E. Pennings, "Optical Multi-Mode Interference Devices Based on Self-Imaging: Principles and Applications," *Lightwave Technology, Journal of*, vol. 13, no. 4, pp. 615–627, apr 1995.
- [16] M. J. Humphrey, "Calculation of Coupling Between Tapered Fiber Modes and Whispering-Gallery Modes of a Spherical Microlaser," Ph.D. dissertation, University of Maryland, College Park, Maryland, 1994.

- [17] A. Rickman and G. Reed, "Silicon-on-insulator optical rib waveguides: loss, mode characteristics, bends and y-junctions," in *Optoelectronics, IEE Proceedings-*, vol. 141, no. 6. IET, 1994, pp. 391–393.
- [18] W. Bogaerts, P. De Heyn, T. Van Vaerenbergh, K. De Vos, S. Kumar Selvaraja, T. Claes, P. Dumon, P. Bienstman, D. Van Thourhout, and R. Baets, "Silicon microring resonators," *Laser & Photonics Reviews*, vol. 6, no. 1, pp. 47–73, 2012.